4-30-2021

CO2-wettability reversal of cap-rock by alumina nanofluid: Implications for CO2 geo-storage

Muhammad Ali

Adnan Aftab

Faisal Ur Rahman Awan
Edith Cowan University

Hamed Akhondzadeh
Edith Cowan University

Alireza Keshavarz
Edith Cowan University

See next page for additional authors

10.1016/j.fuproc.2021.106722
This is an author's accepted manuscript of: Ali, M., Aftab, A., Awan, F. U. R., Akhondzadeh, H., Keshavarz, A., Saeedi, A., ... Sarmadivaleh, M. (2021). CO2-wettability reversal of cap-rock by alumina nanofluid: Implications for CO2 geo-storage. *Fuel Processing Technology, 214,* article 106722. https://doi.org/10.1016/j.fuproc.2021.106722

Authors

Muhammad Ali, Adnan Aftab, Faisal Ur Rahman Awan, Hamed Akhondzadeh, Alireza Keshavarz, Ali Saeedi, Stefan Iglauer, and Mohammad Sarmadivaleh

Highlights:

- Wettability is directly or indirectly related to CO_2 structural trapping potential in cap-rock formation.
- Organic acids have a substantial effect on altering the wettability to CO_2-wet, thus reduced CO_2 trapping potential.
- Alumina Nanoparticles have significantly reversed the wettability to water-wet, thus increased CO_2 trapping potential.

Graphical Abstract

Click here to access/download;Graphical Abstract;GA.png

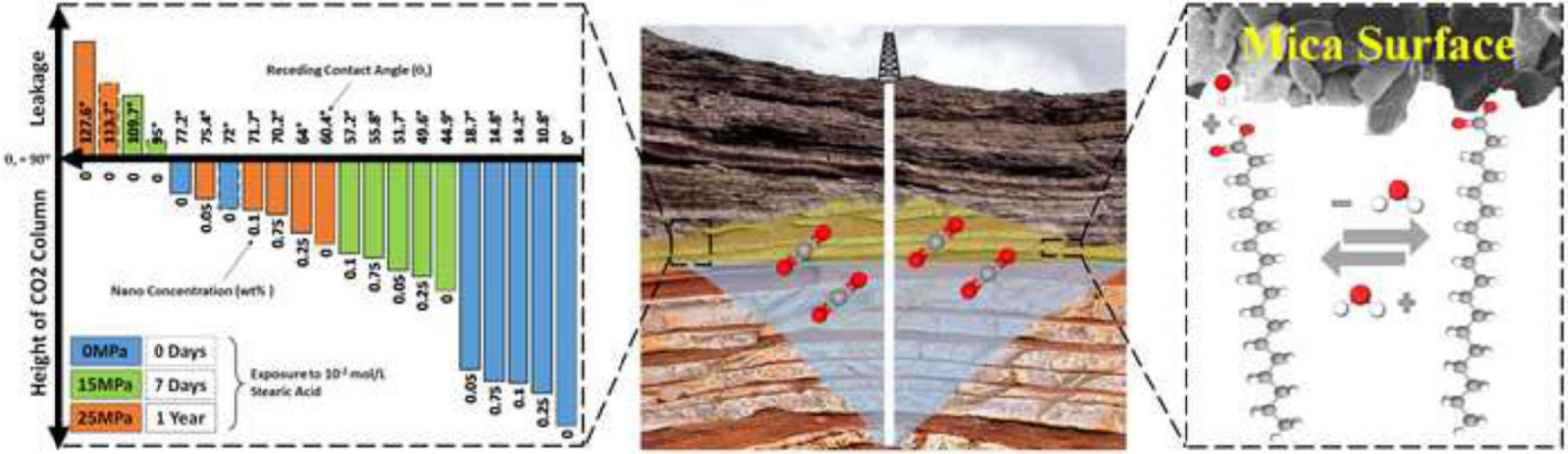

CO_2-Wettability Reversal of Cap-Rock by Alumina Nanofluid; Implications for CO_2 Geo-Storage

Muhammad Ali [a, *], Adnan Aftab [b], Faisal Ur Rahman Awan [c, d], Hamed Akhondzadeh [c], Alireza Keshavarz [c], Ali Saeedi [a], Stefan Iglauer [c], Mohammad Sarmadivaleh [a]

[a] Western Australia School of Mines, Minerals, Energy and Chemical Engineering, Curtin University, 26 Dick Perry Avenue, Kensington, 6151, WA, Australia

[b] Petroleum Engineering Department, Mehran University of Engineering and Technology, Khairpur Mir's Campus, 66020, Sindh, Pakistan

[c] Petroleum Engineering Discipline, School of Engineering, Edith Cowan University, 270 Joondalup Dr, Joondalup, 6027, WA, Australia

[d] Department of Petroleum and Gas Engineering, New M. A. Jinnah Road Ext., Dawood University of Engineering and Technology, Karachi 74800, Pakistan

[*]corresponding author (Muhammad.ali7@postgrad.curtin.edu.au)

Highlights:

- Wettability is directly or indirectly related to CO_2 structural trapping potential in cap-rock formation.
- Organic acids have a substantial effect on altering the wettability to CO_2-wet, thus reduced CO_2 trapping potential.
- Alumina Nanoparticles have significantly reversed the wettability to water-wet, thus increased CO_2 trapping potential.

Abstract

The usage of nanofluids is vast in different applications of nano-energy. These minute nanoparticles can be used to alter the hydrophobicity into hydrophilicity for CO_2-brine-mineral systems in the presence of organic acids. Nonetheless, the literature lacks the information for the behavior of nanoparticles and its associated concentrations in the presence of organic acids at the reservoir (high temperature and high pressure) conditions.

In this study, we have investigated that how different alkyl chain organic acids impact the wettability of mica muscovite for different ageing times (7 days and one year) and how this impact can be reversed by nanofluid priming at different concentrations. To do that, we have used different organic acids with different alkyl chain lengths (hexanoic acid C_6, lauric acid C_{12}, stearic acid $C_{18,}$ and lignoceric acid C_{24}) at 10^{-2} mol/L. We have also used different Al_2O_3 nanoparticle suspensions (0.05 wt%, 0.1 wt%, 0.25 wt% and 0.75 wt%) in deionised water.

When mica substrates were exposed to organic acids for a longer ageing time of 1 year, it has lost its water-wetness rapidly at maximum. Whereas this effect was optimally reduced by 0.25 wt% of alumina nano-formulation and mechanical irreversible adsorption of alumina nanoparticles was noted on mica substrates. This reversal of wettability may raise the containment security and CO_2 structural trapping potential.

Keywords: Alumina Nano-particles, Organic Acids, Wettability, CO_2 Geo-storage, Deep Saline Aquifers, Cap-rock Formation

1. Introduction

CO_2 geo-storage (CGS) sequestration is one of the auspicious technique used to immobilize CO_2 in deep underground formations, thus contributing towards a green environment [1]. To do that, CO_2 is captured from the environment and is stored in deep underground formations. There are many methods that have been previously discussed for CO_2 capture [2-5], but storing CO_2 deep underground formation is an only viable option for permanent CO_2 storage [6-8]. The projection of global CO_2 emissions in 2020 was 36.8 billion tons, which has now decreased by 8% (2.94 billion tons) due to the novel COVID-19 pandemic. This pandemic has caused the forced global industry to shut down, which has led to the sharpest fall of CO_2 emissions since World War II [9]. However, future projection depicts that CO_2 emissions will gain momentum towards 43.08 billion tons by 2050 [10]. The projected amount of CO_2 emissions is at an alarming situation, and if its large portion is not stored in underground formations may lead to accelerated global warming and irreversible climate change [1, 11].

Some of the prime candidates for CO_2 storage are deep saline aquifers, depleted petroleum oil reservoirs, coal beds, basaltic formations, and organic shale reservoirs [1, 12, 13]. These formations have vast storage capacities and can act as a barrier for CO_2 mobilization after its storage to mitigate global warming [1, 6-8, 14]. After CO_2 injection in underground formations, it is restrained by different mechanisms, which comprises of structural trapping (in cap-rock, sandstone, and carbonate formations) [6, 15-18], residual or capillary trapping (in sandstone and carbonate formations) [19-21], dissolution and mineral trapping (in basaltic, sandstone and carbonate formations) [22-25], diffusion and adsorption trapping (in coal bed and organic shale formations) [26-29].

In this context, wetting characteristics (wettability) of CO_2 geo-storage formation govern the storage trapping capacities, containment security, production enhancement, and fluid dynamics

[30-34]. It is shown in previous studies that less water-wet conditions have shown the reduced potential for CO_2 storage [17, 35-38]. However, there is a serious lack of data that can comprehend complex wettability phenomena at realistic storage cap-rock environments. It is proven in the literature that subsurface realistic storage environments are reductive or anoxic in character, which contains highly diluted amounts of organic molecules [39-41]. These minute organic concentrations are sufficient to alter wettability from water-wet to oil-wet [42-44], thus, reducing storage capacities and containment security [7, 14].

In this perspective, alumina nanofluid suspensions can be a vital solution to diminish the effect of reductive conditions in subsurface cap-rock storage formations. It is shown in the literature that nanofluids are positively used for versatile applications of subsurface operations [45], like chemical flooding [46], enhanced oil recovery [47-50], drilling [51-54], low salinity water flooding [55-57], IFT reduction [58], and wettability alteration [8, 59, 60].

We have thus experimented CO_2/brine/Mica (muscovite, cap-rock proxy) contact angles (advancing and receding) to investigate rock wetting characteristics (in the presence of organic acids and alumina nanofluids) for determining CO_2 structural trapping capacities in cap-rock formations. Shale caprock formations contains an abundant mineral called illite that has a similar mineralogical structure like to mica (muscovite), which can be represented as a good caprock proxy [15, 16, 61]. It is already proven in many previous studies that shale samples already contain existing organics in them which has profound impact on wettability studies [27, 62]. Therefore, we have used clean mica muscovite samples (as a proxy of caprock) to obtain the correct thresholds for organic acids. It is also depicted in various previous wettability studies, where mica has been used as a proxy of caprock formation [6, 15, 16]. Muscovite chemically represented as $KAl_2(AlSi_3O_{10})(OH)_2$ [15, 16], and it is commonly present in mica family with other members like, phlogopite, illite, and biotite, [63]. Further, existence of muscovite is well proven in various sedimentary, metamorphic, and sedimentary formations

[64]. Previous studies have proven that these minerals wetting state is closely related with structural trapping capacities [18, 19].

This information will shed light that how mica substrates aged in organic acids alter the wettability to oil-wet, hence reduced CO_2 structural trapping capacity [6] and how these effects can be reversed by ageing organic-aged mica substrates in alumina nanofluids, hence increased CO_2 structural trapping capacity (similar trends were found in sandstone and carbonate formations by using silica nanofluids) [8, 59]. It is vital for CGS projects to account for these organic and alumina nanofluid thresholds for determining project feasibility and reduced uncertainty.

2. Experimental

2.1. Materials

Hydrophilic alumina nanoparticles (Al_2O_3) were acquired from Sigma Aldrich (details are given in Table 1) for formulating different nanofluid suspensions (0.05 wt%, 0.1 wt%, 0.25 wt%, and 0.75 wt%) in de-ionized (DI) water (Ultrapure of electrical conductivity = 0.02 mS/cm from David Gray). Pure mica crystals (dimensions = 15 mm x 20 mm x 3 mm, from Ward's natural science) were used as the proxy of cap-rocks. Ten wt% brine solution was prepared by mixing NaCl (purity ≥ 99.9 mol%, from Rowe Scientific) and deionized water as a proxy of formation water for contact angle measurements.

It is proven in the literature that petroleum and gas reservoirs were the by-product of fossils, which comprise organic acids (from C_4 to C_{26}) [65]. These organic acids are in abundant quantity in depleted oil reservoirs and also occurs in deep saline aquifers due to organic substance diagenesis and biodegradation of fossil mixtures where anaerobic situations flourish [39-41]. In order to mimic the real reservoir situation for depicting the presence of organic

acids in storage formations, we have used four different organic acids (hexanoic acid, lauric acid, stearic acid, and lignoceric acid) ranging from C_6 to C_{24} (purity ≥ 98 mol%, from Sigma Aldrich) for ageing mica substrates, details are explained in Table 1. The reason for choosing equal amount of difference in alkyl chain length of organic acids was to see the effect of alkyl chain length on wettability (explained in detail in section 3.1).

Drops of hydrochloric acid (HCl, the concentration of 37 vol%, from Sigma Aldrich) was introduced in 2 wt% NaCl solution for controlling its pH to 4 pKa and to ionize the mica substrates for speeding the ageing process of organic acids (details are given in section 2.2.2). For removal of contaminants from mica substrates before and after the ageing process, Ultra-pure nitrogen (purity = 99.999 wt%, from BOC, gas code-234) was utilized. Contact angle (advancing and receding) measurements were conducted in CO_2 (purity = 99.999 wt%, from BOC, gas code-082) atmosphere at high pressure and high temperature environments for simulating CO_2 geo-storage conditions. Methanol, toluene, acetone (purity ≥ 99.9 mol%, from Chemlab), and DI water were used to clean away pre-existing contaminations on mica substrates. n-Decane solution (purity ≥ 99.9 mol%, from Sigma Aldrich) was used to formulate various organic acid concentrations as the base liquid.

Table 1. Aluminum Oxide (Al_2O_3) nanoparticles and organic acids details.

Solubility in water	Insoluble
Molar weight (gm/mol)	101.96
Surface area (m^2/gm)	85-115
Particle Size	13 nm
Density (g/cm^3]	3.987
Purity (wt%)	≥ 99.8

Name of Organic Acid	pH (pKa)	Physical state	Formula	Molar mass (g/mol)	Number of C atoms	Chemical Structure
Hexanoic acid	4	Liquid	$C_6H_{12}O_2$	116.158	6	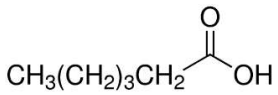
Lauric acid	5.3	solid	$C_{12}H_{24}O_2$	200.318	12	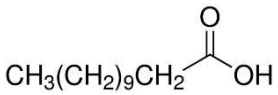
Stearic acid	6	solid	$C_{18}H_{36}O_2$	284.4772	18	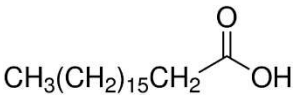
Lignoceric acid	7.4	solid	$C_{24}H_{48}O_2$	368.63	24	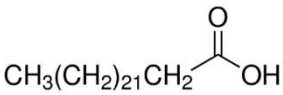

2.2. The procedure of Mimicking Geo-Storage Environments for Mica Surfaces

2.2.1. Initial Cleaning Procedure of Pristine Mica

Pristine mica substrates contain impurities which may affect the experimental results. In order to avoid this, it is pertinent to clean pure mica substrates as they are received. We thus cleaned pure mica samples with deionized water and acetone to eliminate any in-organic or organic surface impurities. This procedure was followed by blow of ultra-pure nitrogen on the substrate's surfaces; as well as a vacuum oven was used for the drying process (80 °C, time = 120 minutes) for removal of any remaining fluid after preliminary cleaning. Afterward, air plasma (Diemer Yocto instrument) was used to treat the mica substrates for 20 minutes to eliminate any residual fragments after the drying procedure [66].

2.2.2. Simulating Mica Substrates as Geo-Storage Formation

CO_2 storage formations are anoxic in character which contains organic impurities that lie in the exposure of formation waters (note this exposure can be for millions of years). Therefore, it is pertinent to simulate a similar mineralogical situation in-order to fully comprehend the

underground physiognomies for the contact angle experiments [67, 68]. There is a serious lack of data in the literature for comprehending the effects of organics on various types of storage formations at various geophysical conditions. However, to do this, silanes were utilized earlier for modifying the hydrophilic surfaces [69], but real reductive conditions for storage formations do not contain silanes (note silanes are highly reactive in reductive conditions). It is previously proven that deep saline aquifers contain enough volume of organics to alter their wettability from water-wet to oil-wet [6, 39-41], and their presence is possible due to organic substance diagenesis and biodegradation of fossil mixtures where anaerobic situations flourish [70, 71]. Therefore, it is more realistic to use organic acids for modifying the wettability of the rock matrix, instead of using silanes at laboratory scale [42, 59]. This modification of mineral hydrophobicity happens due to chemical bonding between hydroxyl groups of mineralogical surfaces and organic esterification [6, 7, 14, 59]. Thus we followed the subsequent approach [67, 68, 72, 73].

Initially, NaCl brine (2 wt%) was formulated with deionized water, and drops of aqueous HCl were added for maintaining the pH at four pKa. Afterward, pristine mica substrates were aged with a solid/liquid ratio of 1:5 in pH-controlled two wt% NaCl brine. This process ionizes the pristine mica substrates in order to increase the adsorption rate of organic acids for mimicking the millions of year's formation water exposure [6, 7, 14, 43, 59, 74]. Thereafter, a blow of ultra-pure nitrogen was used to remove the brine solution from sample surfaces to elude impurities. Consequently, ionized mica substrates were aged in different organic acid/n-decane solutions of prescribed concentration of 10^{-2} mol/L (note four mica substrates were aged in each organic acid for each nanofluid suspension). Our mica substrates remained in organic acid/n-decane solutions for seven days (initial contact angle measurement as a function of ageing) and one year (subsequent contact angle measurement as a function of ageing). This variation in ageing is due to provide enough interval for mimicking formation performance to

accurately comprehend wettability characteristics [8, 67, 68, 75]. However, ageing with 7 days and one year does not show a significant difference in contact angle measurements (explained in section 3.1), this is due to the optimum ageing effect was already achieved in 7 days and longer interval ageing of one year have only caused an insignificant forced ageing resulting in less contact angle differences between 7 days aged samples and one year aged samples.

In-order to contain exact organic acid concentration (10^{-2} mol/L in our case), acrylic containers with tightly sealed caps were used for the ageing process (especially useful in 1-year ageing) to elude n-decane evaporation. This evaporation can cause a change in organic concentration and subsequent error in comprehending the exact wettability threshold. Afterward, acrylic containers were stored in a closed environment (fume hood) to elude impurities for a year.

2.3. Ageing of Organic Aged Mica Substrates in Alumina Nanofluids

2.3.1. Formulation of Alumina Nano-Fluid

Various concentrations (0.05 wt%, 0.1 wt%, 0.25 wt%, and 0.75 wt%) of alumina nano-formulations were formulated (nanofluid formulation was done by sonication method) in order to comprehend their competence for wettability reversal of CO_2/brine/mica systems. The prescribed weight of Al_2O_3 nano-particles (for various concentrations) was added to deionized water and sonicated (Ultrasonic homogenizer, Frequency 20 kHz, Sonics and Materials Incorporation, USA) for 15 minutes (note that homogeneous stirring is not possible with a magnetic stirrer) [76]. This process is conducted with a micro tip (titanium material) of 9.5 mm diameter with a sonication amplitude of (40 %) and energy of (9500 Joules).

2.3.2. Alumina Nano-Fluid's Stability

It is crucial to determine the stability of nano-formulations, which is a pertinent aspect to comprehend its competence for reversal of wettability [8]. To do this, nanofluid electrical stability phase behavior, i.e., Zeta potential (mV) and average particle size (nm) results for alumina nanoparticles were measured from pH level of 6 to 12 (note same range has been noted in deep saline aquifers [77]. Zeta sizer Nano (Malvern, ZS ZEN 3600, Malvern Instruments, UK) was employed for each nanofluid concentration (0.05 to 0.75 wt%), while pH was measured using a pH meter (resolution 0.01 pH, Ohaus, Australia).

Lower Zeta potential values (+ 10 to -10 mV) of the nano-formulation are incipiently electrically stable and are prone to aggregate quicker than as compared to higher values (i.e., Absolute zeta potential > 35 mV) [78, 79]. Furthermore, the repulsive forces (positive or negative charged) are significantly decreased, resulting in acceleration of the nanoparticle coagulation process that yields sedimentation in the presence of the electrolyte. Cationic and anionic surfactants can alter the electrical stability (i.e., zeta potential) of the particles (in the present case, alumina nanoparticles) by coating particle's surface with their counter-ion head group, hence resulting in supercharged particles [80, 81].

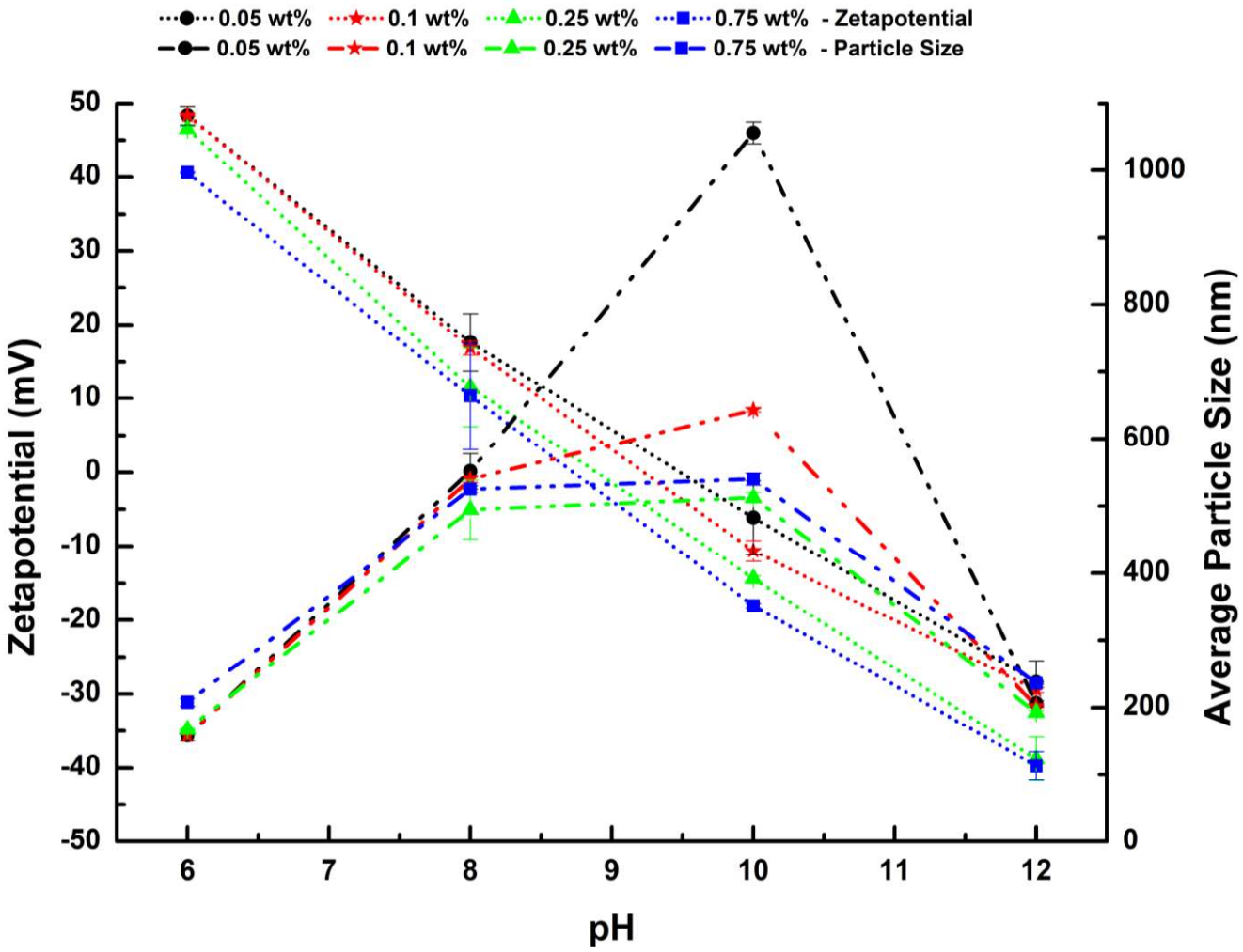

Figure 1. Zeta potential and average particle size measurements of various alumina nano-particles concentration (0.05, 0.1, 0.25 and 0.75 wt%) as a function of pH.

The zeta potential measurement depicts that the alumina nanoparticles have an isoelectric point (IEP, i.e., $\zeta=0$) at a pH level of 8 to 10 in DI water, as shown in Figure 1. It is noteworthy to mention here that, as the weight percentage is increased from 0.05 to 0.75, a decline in zeta-potential on the positive side is observed (e.g., at pH = 6), however when we observe on the highly alkaline side (i.e., pH = 12) an inverse phenomenon is observed. This change of behavior is due to OH^- ions added to the nano-formulation. As more alumina nanoparticle adsorptive sites at more significant loading (i.e., 0.75 wt%), the more OH^- gets attached to the nanoparticle

surface, hence resulting in higher dispersion stability [79]. Generally, the data shows that with increasing concentration of nanofluids, the average particle size (d_{av}) has increased (up to 10 pH). However, upon a further increase in pH, the d_{av} has decreased owing to the enhancement of electrostatic repulsion due to the absorption of OH^- ions, also resulting in higher zeta potential value (on the positive side).

Alumina nanofluid is an excellent candidate for muscovite owing to its broad spectrum of zeta potential (i.e., from 48 to -40 mV) and its associated stability across a wide pH range (i.e., from 6 to 12 pH), as can be seen in Figure 1. The absolute difference in surface roughness owing to the presence of nanoparticles can be examined quantitatively, as can be seen in Table 2. It is hypothesized that alumina nanoparticles are chemisorbed onto the muscovite surface due to its surface activity, as can be seen in Figure 1, for which the presence of OH^- charges plays a vital role in interacting with positively charge mica surface.

2.3.3. Ageing Procedure of Organic Aged Mica Substrate's in Alumina Nano-Fluids

It is proven in the literature that nanofluids have considerable competence in comprehending wettability reversal [8, 47-49]. To do this, organic/n-decane aged mica substrates were vertically submerged (note vertical submerging of mica samples reduces gravitational deposition of nanoparticles) for 5 hours in various alumina nano-formulations (0.05 wt%, 0.1 wt%, 0.25 wt%, and 0.75 wt%) at elevated temperature 323 K and atmospheric pressure to form nano-modified mica surfaces. This ageing is obtained with a solid/nanofluid ratio of 1:5 (1 gram of mica substrate for 5 grams of nano-formulation) for delivering the same coverage for each mica surface [8, 59].

Mechanistically, the nanofluid ageing process provides a very strong chemical reaction by the ageing of the hydroxyl group of nano-formulation with a hydroxyl group of mica substrate

(note this chemical reaction is the reason of irreversible adsorption of nanoparticles on mica substrates). This irreversible adsorption of nanoparticles on organic/n-decane aged mica substrates is responsible for shifting the hydrophobicity into hydrophilicity. Previously, quartz substrates aged in organic acids were placed in negatively charges SiO_2 nanoparticle solutions, which has shown similar significant wettability reversal to water-wet [8, 59].

Overall, the hydroxyl group of mica substrates is esterified with organic acids in a condensation reaction (shifting the wettability to CO_2-wet), and nanoparticles cause irreversible adsorption on organic/n-decane aged mica substrates in a chemical reaction (reversing the wettability to weakly water-wet).

2.4. Characterization of Nano-aged, Organic-aged, and Pristine Mica substrates

2.4.1. Surface Chemistry

Surface elemental analysis (in wt%) of each mica sample was carried out using a Field Emission Scanning Electron Microscope (FESEM) from Oxford Instruments via energy dispersive spectroscopy (EDS) technique. These measurements were done on all pure, organic/n-decane aged and nano-aged mica substrates. It is clear from our results that the ageing of organic acids and nano-formulations have a significant effect on the surface elemental analysis (average elemental values of pure, organic-aged, and nano-aged mica substrates are depicted in Table 2). A significant average increase in surface alumina concentration (+19.1 wt% Al, for Hexanoic-aged surface, +17.4 wt% Al, for Lauric-aged surface, +21.4 wt% Al, for Stearic-aged surface, and +18.5 wt% Al, for Lignoceric-aged surface) due to adsorption of nanoparticles [8] and in surface carbon concentration (+6.1 wt% C, for Lignoceric Acid, +4.5 wt% C, for Stearic Acid, +3.8 wt% C, for Lauric Acid and +2.6 wt% C, for Hexanoic Acid) due to chemisorption of carboxylic acids was noted on mica

substrates [6, 72]. These values are the average of 5 data points for each, pure, organic-aged, and nano-aged mica substrates (A detailed surface elemental analysis is given in Table S1). Further, high magnification scanning electron micrographs (SEM) were acquired on pure and nano-aged mica substrates for depicting the irreversible adsorption of nano-formulations (Figure 2, it is clearly shown that 0.25 wt% Alumina nano-formulation have uniformly adsorbed on mica substrate). Such uniform adsorption of nano-formulation is responsible for wettability reversal from a strongly hydrophobic surface to a weakly hydrophilic surface. "±" shows standard deviation in all mica substrates tested in that particular range (Table 2).

Table 2. Average surface elemental analysis of pristine, organic-aged, and nano-aged mica substrates*.

Organic Acids	Average elemental values of pristine mica					Average elemental values after organic-aged mica (10^{-2} mol/L)					Average elemental values after nano-aged mica (0.05 wt%, 0.1 wt%, 0.25 wt% and 0.75 wt%)				
	wt% Al	wt% Si	wt% C	wt% O	wt% K	wt% Al	wt% Si	wt% C	wt% O	wt% K	wt% Al	wt% Si	wt% C	wt% O	wt% K
Hexanoic acid	19.4 ± 0.8	21.9 ± 1.0	3.2 ± 0.4	46.9 ± 0.5	8.7 ± 0.6	18.7 ± 1.1	20.5 ± 1.7	5.7 ± 0.4	47.8 ± 3.0	7.4 ± 0.7	37.8 ± 7.4	13.2 ± 3.8	4.8 ± 0.5	38.4 ± 3.0	5.8 ± 0.5
Lauric acid	19.3 ± 0.9	22.3 ± 0.7	2.8 ± 0.3	47.1 ± 1.3	8.5 ± 0.6	18.6 ± 0.6	19.9 ± 1.4	6.6 ± 0.3	47.6 ± 1.0	7.4 ± 1.0	35.9 ± 8.9	13.3 ± 3.3	5.3 ± 0.4	39.9 ± 5.5	5.6 ± 0.6
Stearic acid	19.5 ± 0.8	22.2 ± 1.5	3.2 ± 0.7	46.6 ± 0.8	8.6 ± 0.8	18.5 ± 0.9	20.5 ± 1.5	7.7 ± 0.3	45.8 ± 1.5	7.5 ± 0.7	40.0 ± 8.6	11.7 ± 3.2	5.9 ± 0.2	36.5 ± 5.2	6.0 ± 0.5
Lignoceric acid	19.4 ± 0.7	22.4 ± 1.2	3.1 ± 0.6	46.4 ± 1.2	8.8 ± 0.5	18.8 ± 1.1	20.3 ± 0.5	9.1 ± 0.2	44.6 ± 1.8	7.2 ± 0.7	37.3 ± 8.9	13.2 ± 2.6	6.8 ± 0.4	37.1 ± 5.4	5.7 ± 0.6

* Average of 5 data points of each, pure, organic-aged, and nano-aged mica substrates of four different organic acids (hexanoic, lauric, stearic, and lignoceric acid) and four different nano-formulations (0.05 wt%, 0.1 wt%, 0.25 wt%, and 0.75 wt%).

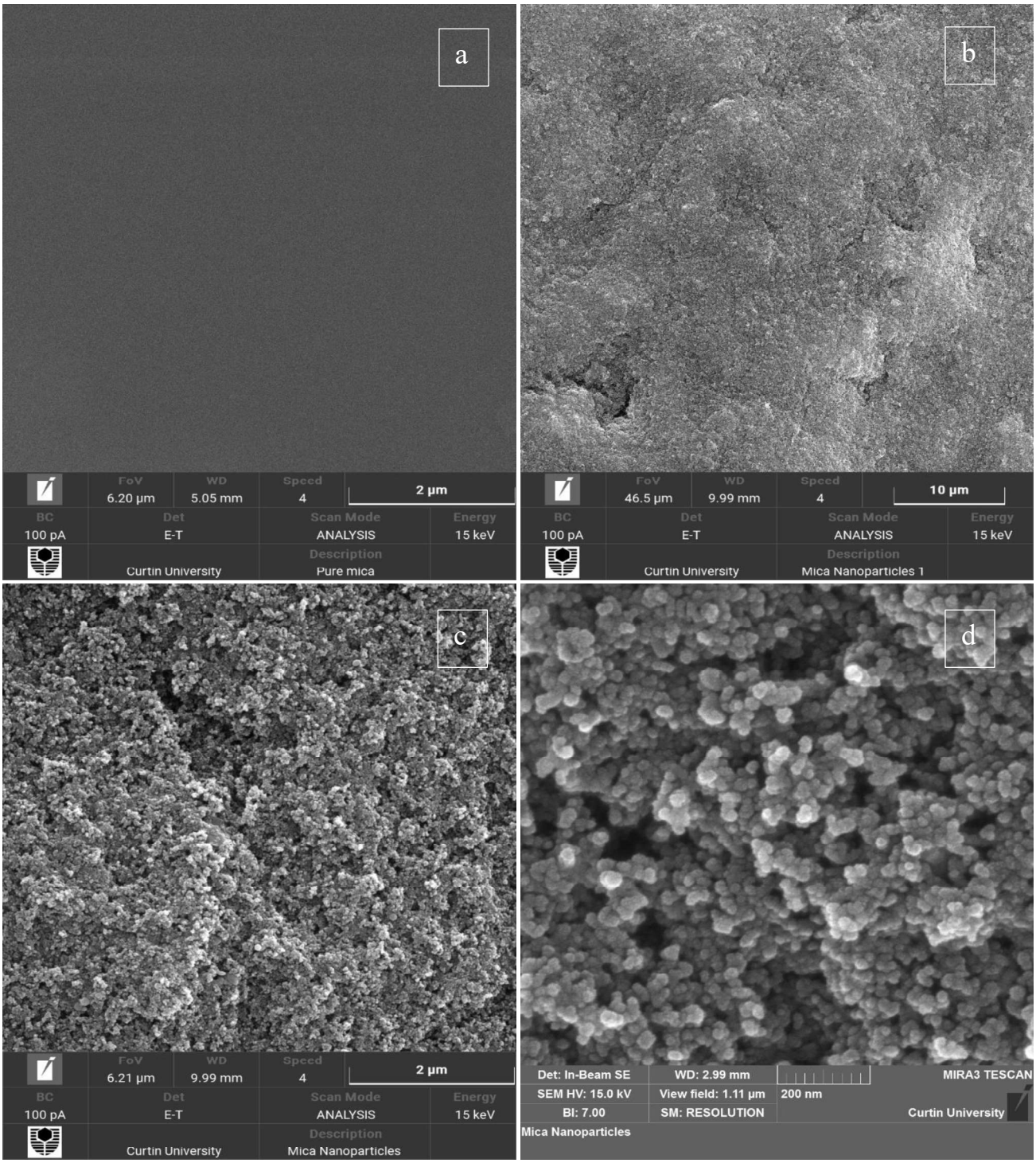

Figure 2. Different magnifications of SEM Micrographs (a) Pristine mica at a magnification of 2 µm (b) 0.25 wt% Alumina nano-aged mica surface at a magnification of 10 µm (c) 0.25 wt% Alumina nano-aged mica surface at a magnification of 2 µm (d) 0.25 wt% Alumina nano-aged mica surface at a magnification of 200 nm.

2.4.2. Surface Roughness

Surface roughness has a substantial impact on contact angle measurements, hence wettability [82]. Therefore, all substrates (pristine mica, organic-aged mica, and nano-aged mica) were characterized by conducting surface topography (Atomic force microscopy by Flex-Axiom, Controller C3000 AFM instrument from Nano-surf) measurements. Topographic experiments have revealed that pristine mica substrates have a very smooth surface (route mean square, RM), ranging from 1 to 2 nm [6]. Further, the topography of organic-aged and nano-aged mica substrates have also depicted homogenous and smooth surfaces with an average root mean square ranging from 200 to 460 nm (for organic-aged mica) [6] and 340 to 620 nm (for nano-aged mica). It is proven in the literature that surfaces with average route mean square roughness for more than 1 μm has a considerable effect on wettability measurements [83]. Hence, all mica substrate's surface roughness resulted in less than 1 μm value; therefore, roughness has no impact on contact angle experiments [84].

2.5. Contact Angle Experiments

There are several methods to quantify wettability behavior, like, capillary pressure and relative permeability curve, nuclear magnetic resonance (NMR) technique, spinning drop technique, Wilhelmy balance, and capillary rise method, Amott-Harvey index, and US Bureau of Mines (USBM) core flood method. All these methods can give indirect wettability calculation, whereas, contact angle method is the only method that gives direct quantitative wettability calculation in a given rock fluid system [8, 16-18, 59]. This method contains a tilted surface technique for the calculation of advancing (θ_a) and receding (θ_r) contact angles [85].

In this technique (Figure 3), a flat mineral sample surface (mica in our case) is placed inside the high pressure and high temperature cell (HPHT, Hastelloy material made) on a tilted plate.

342 For a relative rock fluid system, it is pertinent to obtain thermodynamically equilibrated brine
343 solution with CO_2 and mica substrates. Mica is a reactive surface which can react in acidic
344 environments due to the presence of CO_2 [86, 87], causing errors in wettability experiments.
345 Therefore, brine solution is introduced in Parr reactor mixed with CO_2 and mica substrates at
346 desired experimental (high pressure and high temperature) conditions to obtain thermodynamic
347 equilibration before the contact angle measurements [88]. Thereafter, gas (CO_2 in our case) is
348 introduced into the HPHT cell at desired reservoir conditions (323 K, 0.1 MPa, 15 MPa, and
349 25 MPa in our case) controlled by a high precision syringe pump (Teledyne ISCO, Model D-
350 500, pressure accuracy of 0.1%). Afterward, a drop of thermodynamically equilibrated brine
351 (average drop size was 4.5 μL ± 0.75 μL) is dispensed (controlled by another high precision
352 syringe pump) on the tilted mineral surface. This process is video recorded for determining
353 advancing (θ_a) and receding (θ_r) contact angles at the front and back edges of the brine droplet
354 [43]. The schematic of the HPHT contact angle system is depicted in (Figure 3). A further
355 detailed description of this process is given in our previous articles [6-8, 14].

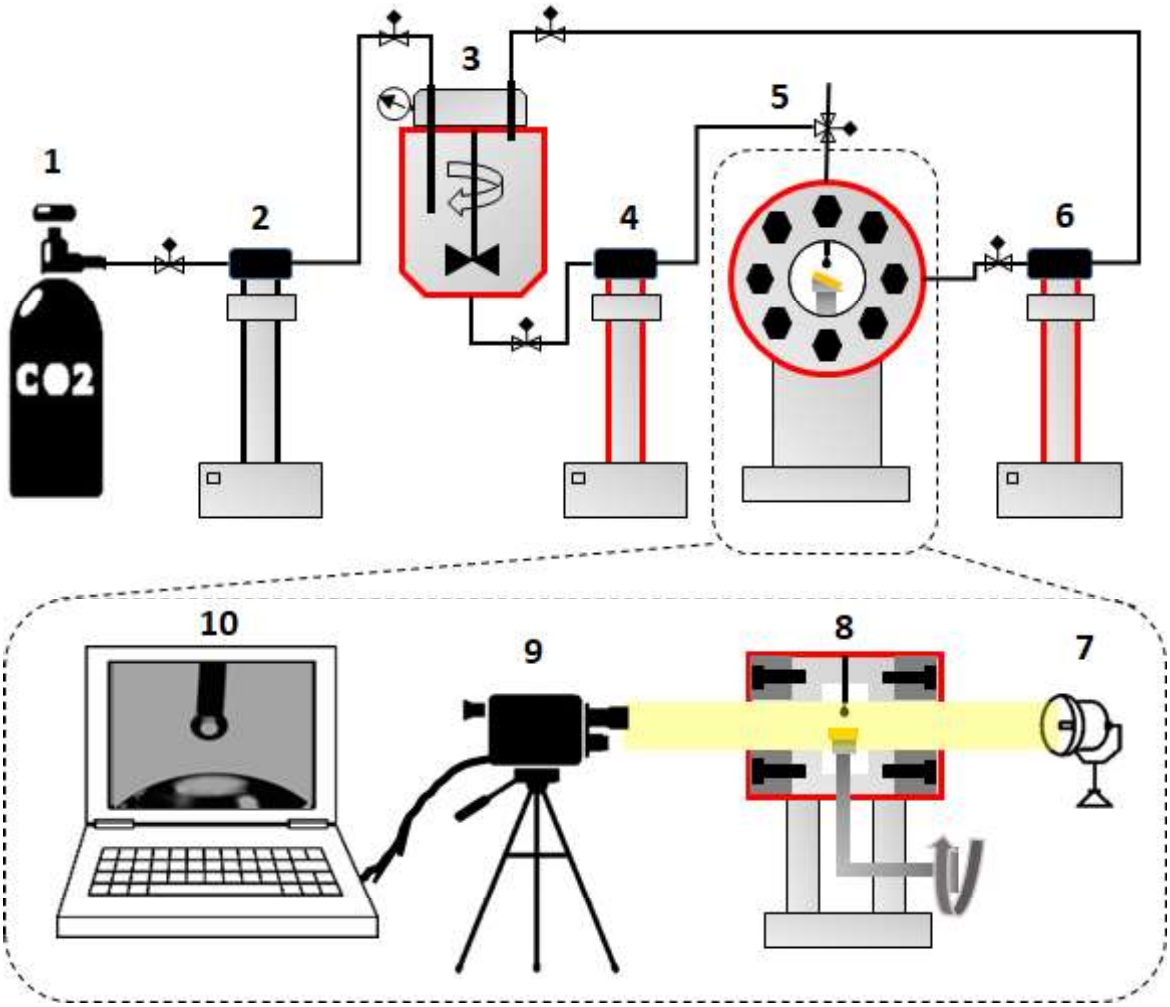

Figure 3. Schematic of HPHT contact angle system (1) CO_2 bottle (2) ISCO syringe pump for CO_2 (3) High-pressure Parr reactor for live brine formulation (4) ISCO syringe pump for live brine (5) HPHT Hastelloy cell with tilted plate housing, front view (6) ISCO syringe pump for wet CO_2 (7) Light projection (8) HPHT Hastelloy cell with tilted plate housing, side view (9) High-resolution video camera (10) ImageJ software for interpretation.

3. Results and Discussion

It is pertinent to comprehend the quantitative assessment of CO_2-wettability for cap-rock formations (mica in our case). This assessment is crucial for determining the CO_2 drive and its distribution across the storage formation [24, 35], storage capacities [16, 17], flow properties

[18, 89], and containment security [90]. In this regard, capillary outflow can happen when the receding contact angle of brine (10 wt% NaCl in our case) is greater than 90° (this phenomenon represents CO_2 injection into the storage formation while displacing water), thus reduced structural trapping capacity [31]. Whereas, wettability have no impact on primary drainage when the advancing contact angle of brine is less than 50° (this phenomenon represents water injection into the storage formation to capillary trap CO_2) [38, 61]. It is also proven that dissolution trapping is substantially impacted by CO_2-wettability alteration [22, 23].

It is clear from our contact angle measurements that hydrophilic mica surfaces were greatly affected by the presence of organic acids and rapidly lost their water-wetness. This wettability alteration can greatly affect the structural trapping capacities of mica cap-rock, whereas this wettability shift can be reversed by alumina nanofluid treatment. Initially, pristine mica substrates were tested at atmospheric pressure and elevated temperature (323 K), which resulted in a completely hydrophilic state with $\theta = 0°$ [6, 15, 16]. Whereas, reservoir conditions (323 K, 15 MPa and 25 MPa) have depicted weakly water-wet state ($\theta_a = 50.2° \pm 3°$ and $\theta_r = 44.9° \pm 3°$ at 15 MPa; and $\theta_a = 65.1° \pm 5°$ and $\theta_r = 60.4° \pm 5°$ at 25 MPa) [6, 15, 16].

3.1. Effect of Organic Acids as a function of Ageing Time, alkyl chain length and Pressure on CO_2 Geo-Storage Capacities

CO_2-wettability of cap-rock formation is directly or indirectly related to CO_2 structural trapping capacity. In ideal situations, wettability drives the ability of CO_2 to displace the water and induce below the cap-rock formation. This happens when CO_2 move up-ward (due to buoyancy factor) and apply force on solid cap-rock formation; thus, structurally trapping itself. However, in real situations, organic fatty acids are present in the storage formation, which can significantly affect the wettability, thus, causing capillary leakage [6, 40, 41].

Our results have shown that at a constant organic acid (hexanoic acid C_6, lauric acid C_{12}, stearic acid C_{18}, and lignoceric acid C_{24}) concentration of 10^{-2} mol/L with different ageing times (7 days and one year), mica has greatly lost its water-wetness. For instance, at a constant pressure of 15 MPa and 323 K for lignoceric acid with one-year ageing time, mica/CO_2/brine contact angles were strongly hydrophobic (θ_a = 131.3° and θ_r = 123.6°) and at similar conditions, with seven days ageing time contact angle values were (θ_a = 115.7° and θ_r = 107.3°) compared to pristine mica (θ_a = 50.2° and θ_r = 44.9°), which may have serious consequences in structural trapping capacities due to prolonged exposure of organic acids (Figure 4).

However, irrespective of ageing time, longer alkyl chain (higher number of carbon atoms) organic acids have a more negative effect on structural trapping (increased contact angle values) compared to shorter alkyl chains (fewer number of carbon atoms) organic acids. Therefore, mica substrates aged in lignoceric acid (C_{24}) have shown higher contact angle values compared to mica substrates aged in hexanoic acid (C_6). For instance, at 25 MPa and 323 K, with an ageing time of one year, of all organic acids (hexanoic acid C_6, lauric acid C_{12}, stearic acid C_{18}, and lignoceric acid C_{24}), receding contact angle values were, θ_r = 105.7°, 116.2°, 127.6°, and 136.2°, respectively (Figure 4). Such higher contact angle values can significantly reduce structural trapping capacities (note structural leakage is possible at $\theta_r > 90°$) [6, 16-18].

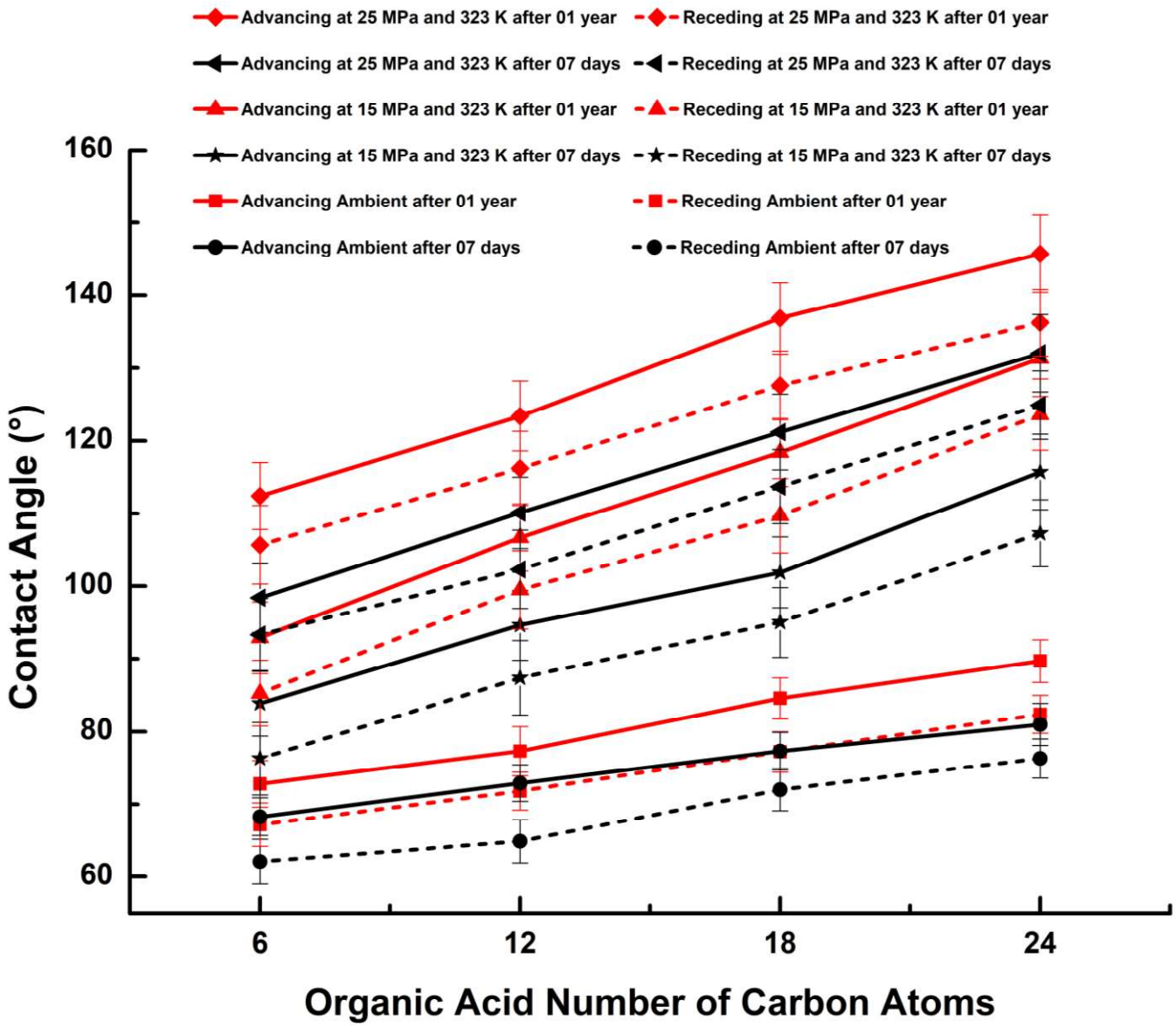

Figure 4. Mica/CO_2/Brine advancing and receding contact angles as a function of ageing time, different organic acids, and pressure.

Further, irrespective of ageing time and type of organic acid, higher pressure (deep saline aquifers > 15 MPa) may cause higher threat (increasing contact angle values) for structural trapping capacities due to an increase in intermolecular forces between solid (mica in our case) and gas (CO_2 in our case) with increasing pressure [91]. For example, mica substrates aged in stearic acid at atmospheric pressure and elevated temperature (323 K) with seven days ageing

time have shown weakly intermediate-wet state θ_a = 72.9° and θ_r = 64.9°, whereas, at similar conditions with higher pressure of 25 MPa, mica/CO_2/brine contact angle values turned in CO_2-wet θ_a = 110.1° and θ_r = 102.3° (Figure 4). Hence, such minute concentrations of organic acids and higher pressures are always present in storage formations; lower structural trapping capacities may be encountered than estimated [7, 39, 70, 71].

3.2. Effect of Nano-Fluids on CO_2 Geo-Storage Capacities

It is shown in the literature that various parameters like temperature, pressure, brine salinity, and organic acids have a substantial impact on CO_2 geo-storage [15, 16, 89]. However, there is a serious lack of data for comprehending the effect of nanoparticles (type and concentration) at HPHT reservoir conditions for CO_2-wettability, hence CO_2-storage capacities. To do that, we have used different concentrations of alumina nanoparticles (0.05 wt%, 0.1 wt%, 0.25 wt%, and 0.75 wt%) in deionized water for the reversal of hydrophobic mica surfaces. Organic-aged mica substrates were aged vertically in these nanofluid concentrations for 5 hours, followed by contact angle measurements at reservoir conditions (323 K, 0.1 MPa, 15 MPa, and 25 MPa in our case). This nano-treatment of mica substrates is achieved by the adsorption efficiency of alumina nanoparticles and their associated concentrations. It is depicted from our results (figure 5 and 6, advancing and receding contact angles with alumina nanofluid) that the wettability of organic-aged CO_2-wet mica substrates have substantially reduced by alumina nanofluid ageing (note the degree of wettability reversal was different for different alumina nanofluid concentrations) [92].

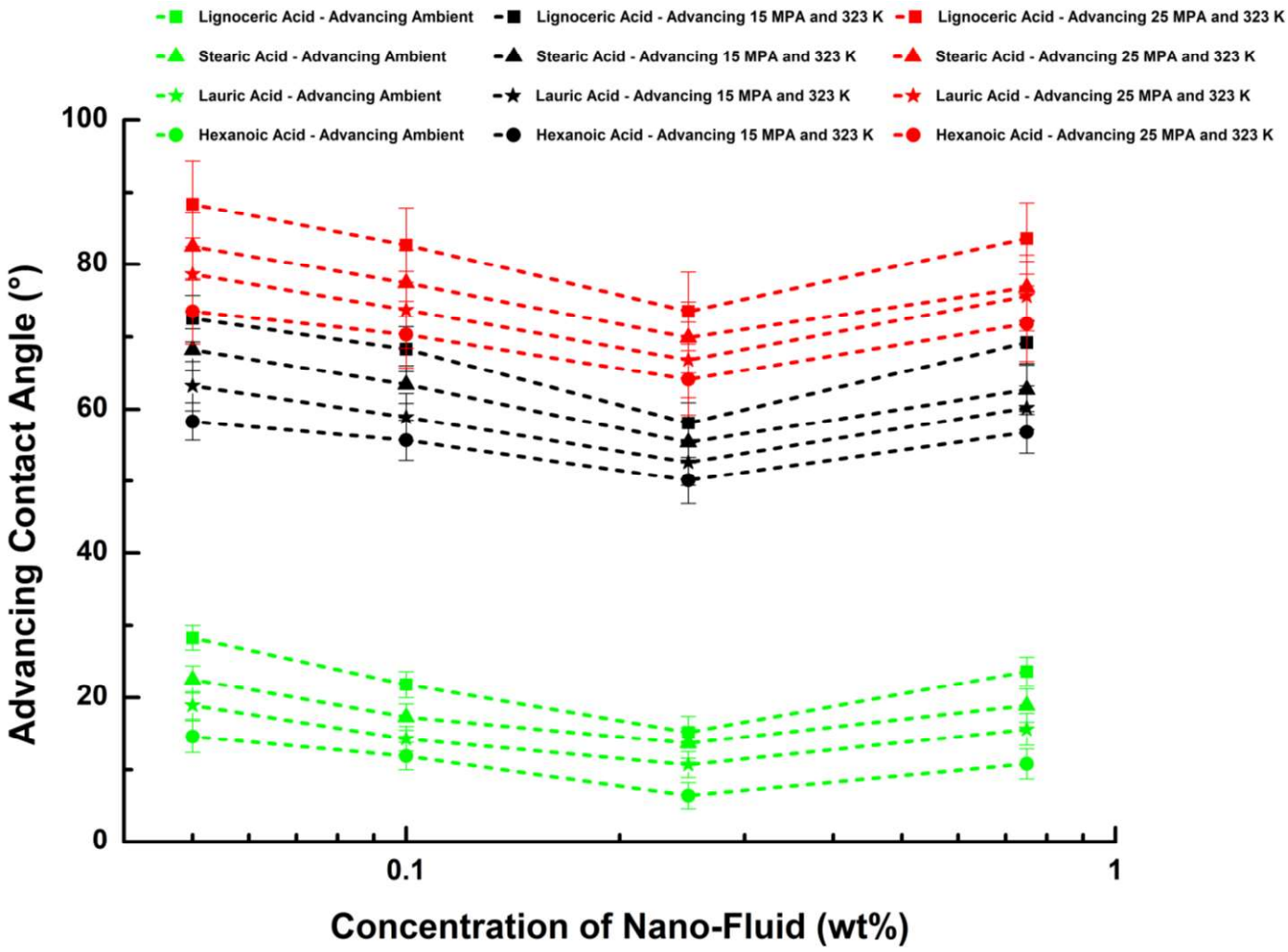

Figure 5. Mica/CO_2/Brine contact angles (advancing) as a function of pressure and different alumina nanofluid concentrations.

For instance, with lignoceric-aged mica substrates at 323 K and 25 MPa for 0.05 wt%, 0.1 wt%, 0.25 wt%, and 0.75 wt% nanofluid alumina concentrations, brine receding contact angles were $\theta_r = 81.6°$, 75.8°, 68.9°, and 76.9°, respectively (note structural trapping limit is $\leq 90°$), which has reduced from $\theta_r = 136.2°$ for lignoceric-aged mica substrates at 323 K and 25 MPa for one-year ageing. It can be seen from the acquired data that each concertation of alumina nanofluid is setting the same trend for other organic-aged mica substrates; however, 0.25 wt% alumina

nanofluid concentration has shown the optimum reversal of wettability as compare to other alumina nanofluid concentrations tested.

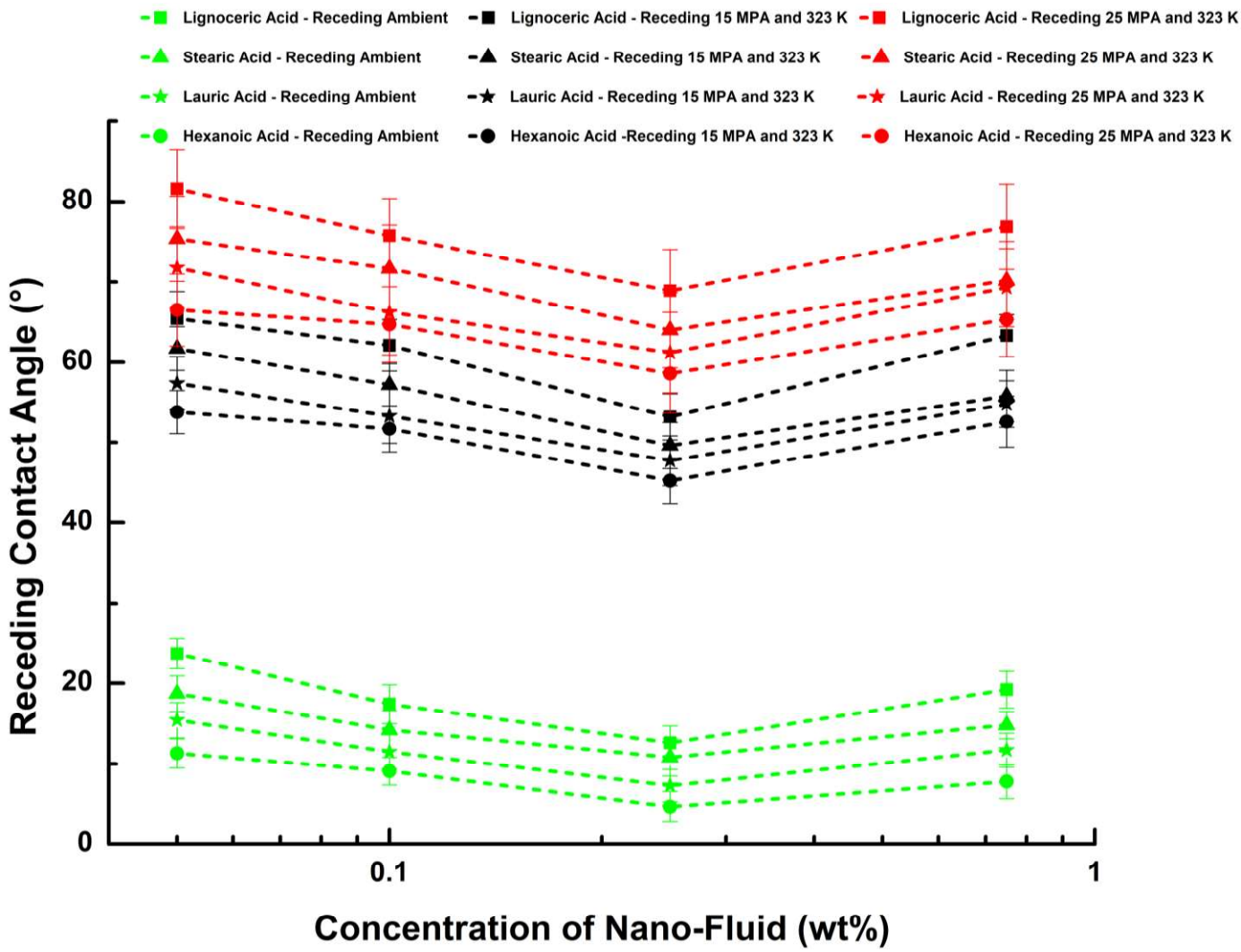

Figure 6. Mica/CO_2/Brine contact angles (receding) as a function of pressure and different alumina nanofluid concentrations.

4. Implications

The conducted contact angle experiments have depicted that the existence of organic acids into CO_2 geo-storage formations (mica in our case) is responsible for shifting the wettability to more CO_2-wet, thus, reduced structural trapping capacities [6, 18]. Therefore, optimum

alumina nanofluid concentration (0.25 wt% in deionized water) is recommended for the reversal of wettability from hydrophobicity to hydrophilicity, hence, increased structural trapping capacities, as depicted in similar studies for applications of SiO_2 nanoparticles in quartz formation [8]. This can be achieved by following two processes.

1. Initially, by injecting optimum nanofluid suspension (0.25 wt% in deionized water) in CO_2-geo storage formation to alter the wettability, which is CO_2-wet due to the presence of organic acids (hence less CO_2 structural trapping potential). This will change its wetting characteristics to Intermediate-wet (hence greater CO_2 structural trapping potential).
2. Finally, when wetting characteristics are shifted towards intermediate-wet, CO_2 will be injected at above supercritical pressure, which will exert the pressure on wetting phase (formation water) and free CO_2 will move upward due to the buoyancy force and will accumulate below the impermeable layer, where it will be structurally trapped below the caprock formation.

Consequently, alumina nanofluid injection may play an integral part as part of CO_2 geo-storage feasibility. Therefore, CO_2 geo-storage projects should account for the strategies where leakage risk can be minimized.

5. Conclusion

Various factors such as formation heterogeneity, brine salinity, temperature, surface roughness, and pressure are basic fundamentals that drive CO_2-wettability of storage formations [14, 16, 55-57, 83, 89, 93, 94]. Nonetheless, organic acids' existence in storage formation is well-proven, which may significantly reduce structural trapping capacities [6, 7, 14, 43], and this may be reduced with different concentrations of nano-fluids in nano-energy applications [8,

47-49, 59]. There is a serious lack of data in the literature that can account for the CO_2-wettability in the existence of organic acids for mitigating project achievability, technical injection problems, containment security, and structural trapping feasibility in cap-rock formation [7, 12, 14, 17, 18, 35, 43]. In contrast, many studies of storage formations have already shown the presence of organics at a larger scale [7, 39-42, 73, 74].

In order to properly address this issue. We have used four organic acids (hexanoic, lauric, stearic, and lignoceric acid) at a fixed organic acid/n-decane concentration of 10^{-2} mol/L with different exposure durations (7 days and one year) for ageing pure mica substrates. Thereafter, different concentrations (0.05 wt%, 0.1 wt%, 0.25 wt%, and 0.75 wt%) of alumina nanofluids were formulated with deionized water for ageing (5-hour duration) organic-aged mica substrates. Contact angle measurements (advancing and receding) were conducted at various storage conditions (323 K, 0.1 MPa, 15 MPa, and 25 MPa) in-order to fully comprehend the wetting characteristics of organic-aged and nano-aged mica substrates, thus, determining structural trapping limits (leakage can occur at > 90°) in the presence of organic acids and nanofluids.

Our results depict that pristine mica substrates were weakly water-wet (θ_a = 65.1° and θ_r = 60.4°) at typical storage conditions (323 K, 25 MPa), which turned strongly hydrophobic (θ_a = 145.7° and θ_r = 136.2°) in the presence of 10^{-2} mol/L lignoceric acid concentration (longer alkyl chain) at similar conditions of 1-year ageing duration (such a change is attributed to chemisorption of organic acids, thus reduced structural trapping potential). However, optimum alumina nanofluid concentration (0.25 wt%) have shown a significant reduction in CO_2-wettability and turned them weakly water-wet (θ_a = 73.5° and θ_r = 68.9°), thus, increased structural trapping potential.

In a nutshell, it is crucial to fully comprehend the CO_2-wettability of cap-rock storage formations in the presence of organic acids and nanofluids at typical storage conditions, as lower structural trapping potential may be predicted, which can affect the feasibility of long term CO_2 geo-storage projects. We thus recommend that CO_2 geo-schemes and simulation strategies should account for the benefits of nano-energy applications into CO_2 geo-storage formations to further de-risking the project viability of CO_2 geo-sequestration.

Conflicts of Interest

There are no conflicts to declare.

Acknowledgments

The first author acknowledges the scholarship (Research Training Program Stipend – 2018) provided by Australian Government for his higher studies, as well as Curtin University for supervision and resources.

Supporting Information

Supporting information accompanies this article, where Energy Dispersive Spectroscopy (EDS) results for each pristine mica, organic-aged mica and nano-aged mica substrates (Table S1), are included.

References

[1] B. Metz, O. Davidson, H. De Coninck, Carbon dioxide capture and storage: special report of the intergovernmental panel on climate change, Cambridge University Press, 2005.

[2] H. Abdolahi-Mansoorkhani, S. Seddighi, CO2 capture by modified hollow fiber membrane contactor: Numerical study on membrane structure and membrane wettability, Fuel Processing Technology, 209 (2020) 106530.

[3] H. Li, M. Qu, Y. Hu, High-temperature CO2 capture by Li4SiO4 adsorbents: Effects of pyroligneous acid (PA) modification and existence of CO2 at desorption stage, Fuel Processing Technology, 197 (2020) 106186.

[4] F. Dietrich, G. Schöny, J. Fuchs, H. Hofbauer, Experimental study of the adsorber performance in a multi-stage fluidized bed system for continuous CO2 capture by means of temperature swing adsorption, Fuel Processing Technology, 173 (2018) 103-111.

[5] N. Wang, Y. Feng, L. Liu, X. Guo, Effects of preparation methods on the structure and property of Al-stabilized CaO-based sorbents for CO2 capture, Fuel processing technology, 173 (2018) 276-284.

[6] M. Ali, A. Aftab, Z.U. Arain, A. Al-Yaseri, H. Roshan, A. Saeedi, S. Iglauer, M. Sarmadivaleh, Influence of Organic Acid Concentration on Wettability Alteration of Cap-Rock: Implications for CO2 Trapping/Storage, ACS Appl Mater Interfaces, 12 (2020) 39850-39858.

[7] M. Ali, S. Al-Anssari, M. Arif, A. Barifcani, M. Sarmadivaleh, L. Stalker, M. Lebedev, S. Iglauer, Organic acid concentration thresholds for ageing of carbonate minerals: Implications for CO2 trapping/storage, Journal of colloid and interface science, 534 (2019) 88-94.

[8] M. Ali, M.F. Sahito, N.K. Jha, Z.U. Arain, S. Memon, A. Keshavarz, S. Iglauer, A. Saeedi, M. Sarmadivaleh, Effect of nanofluid on CO2-wettability reversal of sandstone formation; implications for CO2 geo-storage, J Colloid Interface Sci, 559 (2020) 304-312.

[9] IEA, Global Energy Review 2020, IEA, Paris, (2020).

[10] R. Newell, D. Raimi, G. Aldana, Global Energy Outlook 2019: The Next Generation of Energy, Resources for the Future, (2019) 8-19.

[11] F.M. Orr, Onshore geologic storage of CO2, Science, 325 (2009) 1656-1658.

[12] A.S. Al-Menhali, S. Krevor, Capillary trapping of CO2 in oil reservoirs: Observations in a mixed-wet carbonate rock, Environmental science & technology, 50 (2016) 2727-2734.

[13] X. Ji, C. Zhu, CO2 storage in deep saline aquifers, in: Novel materials for carbon dioxide mitigation technology, Elsevier, 2015, pp. 299-332.

[14] M. Ali, M. Arif, M.F. Sahito, S. Al-Anssari, A. Keshavarz, A. Barifcani, L. Stalker, M. Sarmadivaleh, S. Iglauer, CO2-wettability of sandstones exposed to traces of organic acids: Implications for CO2 geo-storage, International Journal of Greenhouse Gas Control, 83 (2019) 61-68.

[15] M. Arif, A.Z. Al-Yaseri, A. Barifcani, M. Lebedev, S. Iglauer, Impact of pressure and temperature on CO2–brine–mica contact angles and CO2–brine interfacial tension: Implications for carbon geo-sequestration, Journal of colloid and interface science, 462 (2016) 208-215.

[16] M. Arif, A. Barifcani, M. Lebedev, S. Iglauer, Structural trapping capacity of oil-wet caprock as a function of pressure, temperature and salinity, International Journal of Greenhouse Gas Control, 50 (2016) 112-120.

[17] S. Iglauer, A.Z. Al-Yaseri, R. Rezaee, M. Lebedev, CO2 wettability of caprocks: Implications for structural storage capacity and containment security, Geophysical Research Letters, 42 (2015) 9279-9284.

[18] S. Iglauer, C. Pentland, A. Busch, CO2 wettability of seal and reservoir rocks and the implications for carbon geo-sequestration, Water Resources Research, 51 (2015) 729-774.

[19] S. Iglauer, W. Wülling, C.H. Pentland, S.K. Al-Mansoori, M.J. Blunt, Capillary-trapping capacity of sandstones and sandpacks, SPE Journal, 16 (2011) 778-783.

[20] C. Pentland, R. El-Maghraby, A. Georgiadis, S. Iglauer, M. Blunt, Immiscible displacements and capillary trapping in CO2 storage, Energy Procedia, 4 (2011) 4969-4976.

[21] M. Ali, F.U.R. Awan, M. Ali, A. Al-Yaseri, M. Arif, M. Sánchez-Román, A. Keshavarz, S. Iglauer, Effect of Humic Acid on CO2-Wettability of Sandstone Formations, Journal of Colloid and Interface Science, (2020).
[22] S. Iglauer, Dissolution trapping of carbon dioxide in reservoir formation brine–a carbon storage mechanism, in: Mass transfer-advanced aspects, InTechOpen, 2011.
[23] E. Agartan, L. Trevisan, A. Cihan, J. Birkholzer, Q. Zhou, T.H. Illangasekare, Experimental study on effects of geologic heterogeneity in enhancing dissolution trapping of supercritical CO2, Water Resources Research, 51 (2015) 1635-1648.
[24] E.A. Al-Khdheeawi, S. Vialle, A. Barifcani, M. Sarmadivaleh, S. Iglauer, Influence of injection well configuration and rock wettability on CO2 plume behaviour and CO2 trapping capacity in heterogeneous reservoirs, Journal of Natural Gas Science and Engineering, 43 (2017) 190-206.
[25] E.A. Al-Khdheeawi, D.S. Mahdi, M. Ali, C.A. Fauziah, A. Barifcani, Impact of Caprock Type on Geochemical Reactivity and Mineral Trapping Efficiency of CO, in: Offshore Technology Conference Asia, Offshore Technology Conference, 2020.
[26] S. Golding, I. Uysal, C. Boreham, D. Kirste, K. Baublys, J. Esterle, Adsorption and mineral trapping dominate CO2 storage in coal systems, Energy Procedia, 4 (2011) 3131-3138.
[27] M. Arif, M. Lebedev, A. Barifcani, S. Iglauer, Influence of shale-total organic content on CO2 geo-storage potential, Geophysical Research Letters, 44 (2017) 8769-8775.
[28] A. Busch, S. Alles, Y. Gensterblum, D. Prinz, D.N. Dewhurst, M.D. Raven, H. Stanjek, B.M. Krooss, Carbon dioxide storage potential of shales, International journal of greenhouse gas control, 2 (2008) 297-308.
[29] N.S. Kaveh, K. Wolf, S. Ashrafizadeh, E. Rudolph, Effect of coal petrology and pressure on wetting properties of wet coal for CO2 and flue gas storage, International Journal of Greenhouse Gas Control, 11 (2012) S91-S101.
[30] W.G. Anderson, Wettability literature survey-part 4: Effects of wettability on capillary pressure, Journal of petroleum technology, 39 (1987) 1,283-281,300.
[31] D. Broseta, N. Tonnet, V. Shah, Are rocks still water-wet in the presence of dense CO2 or H2S?, Geofluids, 12 (2012) 280-294.
[32] E. Donaldson, W. Alam, Wettability Gulf Publishing Company, Original edition, (2008).
[33] S. Naik, Z. You, P. Bedrikovetsky, Productivity index enhancement by wettability alteration in two-phase compressible flows, Journal of Natural Gas Science and Engineering, 50 (2018) 101-114.
[34] S. Naik, Z. You, P. Bedrikovetsky, Rate enhancement in unconventional gas reservoirs by wettability alteration, Journal of Natural Gas Science and Engineering, 26 (2015) 1573-1584.
[35] E.A. Al-Khdheeawi, S. Vialle, A. Barifcani, M. Sarmadivaleh, S. Iglauer, Impact of reservoir wettability and heterogeneity on CO2-plume migration and trapping capacity, International Journal of Greenhouse Gas Control, 58 (2017) 142-158.
[36] M. Arif, M. Lebedev, A. Barifcani, S. Iglauer, CO2 storage in carbonates: Wettability of calcite, International Journal of Greenhouse Gas Control, 62 (2017) 113-121.
[37] K. Chaudhary, M. Bayani Cardenas, W.W. Wolfe, J.A. Maisano, R.A. Ketcham, P.C. Bennett, Pore-scale trapping of supercritical CO2 and the role of grain wettability and shape, Geophysical Research Letters, 40 (2013) 3878-3882.
[38] T. Rahman, M. Lebedev, A. Barifcani, S. Iglauer, Residual trapping of supercritical CO2 in oil-wet sandstone, Journal of colloid and interface science, 469 (2016) 63-68.
[39] L. Stalker, S. Varma, D. Van Gent, J. Haworth, S. Sharma, South West Hub: a carbon capture and storage project, Australian Journal of Earth Sciences, 60 (2013) 45-58.
[40] D.M. Akob, I.M. Cozzarelli, D.S. Dunlap, E.L. Rowan, M.M. Lorah, Organic and inorganic composition and microbiology of produced waters from Pennsylvania shale gas wells, Applied Geochemistry, 60 (2015) 116-125.
[41] P.D. Lundegard, Y.K. Kharaka, Distribution and occurrence of organic acids in subsurface waters, in: Organic acids in geological processes, Springer, 1994, pp. 40-69.

[42] K.R. Gomari, A. Hamouda, Effect of fatty acids, water composition and pH on the wettability alteration of calcite surface, Journal of petroleum science and engineering, 50 (2006) 140-150.
[43] M. Ali, Effect of Organic Surface Concentration on CO2-Wettability of Reservoir Rock, in, Curtin University, 2018.
[44] S. Iglauer, M. Ali, A. Keshavarz, Hydrogen Wettability of Sandstone Reservoirs: Implications for Hydrogen Geo-Storage, Geophysical Research Letters, (2020).
[45] C. Gu, R. Qiu, S. Liu, Z. You, R. Qin, Shear thickening effects of drag-reducing nanofluids for low permeability reservoir, Advances in Geo-Energy Research, 4 (2020) 317-325.
[46] O.M. Haghighi, G. Zargar, A. Khaksar Manshad, M. Ali, M.A. Takassi, J.A. Ali, A. Keshavarz, Effect of Environment-Friendly Non-Ionic Surfactant on Interfacial Tension Reduction and Wettability Alteration; Implications for Enhanced Oil Recovery, Energies, 13 (2020) 3988.
[47] S. Al-Anssari, M. Ali, S. Memon, M.A. Bhatti, C. Lagat, M. Sarmadivaleh, Reversible and irreversible adsorption of bare and hybrid silica nanoparticles onto carbonate surface at reservoir condition, Petroleum, (2019).
[48] S. Al-Anssari, Z.-U.-A. Arain, A. Barifcani, A. Keshavarz, M. Ali, S. Iglauer, Influence of Pressure and Temperature on CO2-Nanofluid Interfacial Tension: Implication for Enhanced Oil Recovery and Carbon Geosequestration, in: Abu Dhabi International Petroleum Exhibition & Conference, Society of Petroleum Engineers, 2018.
[49] S. Al-Anssari, L. Nwidee, M. Ali, J.S. Sangwai, S. Wang, A. Barifcani, S. Iglauer, Retention of silica nanoparticles in limestone porous media, in: SPE/IATMI Asia Pacific Oil & Gas Conference and Exhibition, Society of Petroleum Engineers, 2017.
[50] Y. Yang, T. Cheng, H. Wu, Z. You, D. Shang, J. Hou, Enhanced Oil Recovery Using Oleic Acid-Modified Titania Nanofluids: Underlying Mechanisms and Oil-Displacement Performance, Energy & Fuels, 34 (2020) 5813-5822.
[51] A. Aftab, M. Ali, M.F. Sahito, U.S. Mohanty, N.K. Jha, H. Akhondzadeh, M.R. Azhar, A.R. Ismail, A. Keshavarz, S. Iglauer, Environmental Friendliness and High Performance of Multifunctional Tween 80/ZnO-Nanoparticles-Added Water-Based Drilling Fluid: An Experimental Approach, ACS Sustainable Chemistry & Engineering, (2020).
[52] M. Ali, H.H. Jarni, A. Aftab, A.R. Ismail, N.M.C. Saady, M.F. Sahito, A. Keshavarz, S. Iglauer, M. Sarmadivaleh, Nanomaterial-based drilling fluids for exploitation of unconventional reservoirs: A review, Energies, 13 (2020) 3417.
[53] A. Aftab, M. Ali, M. Arif, S. Panhwar, N.M.C. Saady, E.A. Al-Khdheeawi, O. Mahmoud, A.R. Ismail, A. Keshavarz, S. Iglauer, Influence of tailor-made TiO2/API bentonite nanocomposite on drilling mud performance: Towards enhanced drilling operations, Applied Clay Science, 199 (2020) 105862.
[54] M. Ali, A. Aftab, Topic review Unconventional Reservoirs Subjects: Energy & Fuel Technology, (2020).
[55] N. Jha, M. Ali, M. Sarmadivaleh, S. Iglauer, A. Barifcani, M. Lebedev, J. Sangwai, Low salinity surfactant nanofluids for enhanced CO2 storage application at high pressure and temperature, in: Fifth CO2 Geological Storage Workshop, European Association of Geoscientists & Engineers, 2018, pp. 1-4.
[56] N.K. Jha, M. Ali, S. Iglauer, M. Lebedev, H. Roshan, A. Barifcani, J.S. Sangwai, M. Sarmadivaleh, Wettability alteration of quartz surface by low-salinity surfactant nanofluids at high-pressure and high-temperature conditions, Energy & Fuels, 33 (2019) 7062-7068.
[57] N.K. Jha, M. Lebedev, S. Iglauer, M. Ali, H. Roshan, A. Barifcani, J.S. Sangwai, M. Sarmadivaleh, Pore scale investigation of low salinity surfactant nanofluid injection into oil saturated sandstone via X-ray micro-tomography, Journal of Colloid and Interface Science, 562 (2020) 370-380.
[58] S. Al-Anssari, Z.-U.-A. Arain, H.A. Shanshool, M. Ali, A. Keshavarz, S. Iglauer, M. Sarmadivaleh, Effect of Nanoparticles on the Interfacial Tension of CO-Oil System at High Pressure and Temperature: An Experimental Approach, in: SPE Asia Pacific Oil & Gas Conference and Exhibition, Society of Petroleum Engineers, 2020.

[59] S. Al-Anssari, A. Barifcani, S. Wang, L. Maxim, S. Iglauer, Wettability alteration of oil-wet carbonate by silica nanofluid, Journal of colloid and interface science, 461 (2016) 435-442.
[60] S. Naik, G. Malgaresi, Z. You, P. Bedrikovetsky, Well productivity enhancement by applying nanofluids for wettability alteration, The APPEA Journal, 58 (2018) 121-129.
[61] P. Chiquet, D. Broseta, S. Thibeau, Wettability alteration of caprock minerals by carbon dioxide, Geofluids, 7 (2007) 112-122.
[62] H. Yu, R. Rezaee, Z. Wang, T. Han, Y. Zhang, M. Arif, L. Johnson, A new method for TOC estimation in tight shale gas reservoirs, International Journal of Coal Geology, 179 (2017) 269-277.
[63] S. Bailey, Classification and structures of the micas, Reviews in Mineralogy and Geochemistry, 13 (1984) 1-12.
[64] C.V. Guidotti, Micas in metamorphic rocks, Micas, reviews in mineralogy, 13 (1984) 357-467.
[65] B. Caballero, L.C. Trugo, P.M. Finglas, Encyclopedia of food sciences and nutrition, Academic, 2003.
[66] S. Iglauer, A. Salamah, M. Sarmadivaleh, K. Liu, C. Phan, Contamination of silica surfaces: Impact on water–CO2–quartz and glass contact angle measurements, International Journal of Greenhouse Gas Control, 22 (2014) 325-328.
[67] J.A. Davis, Adsorption of natural dissolved organic matter at the oxide/water interface, Geochimica et Cosmochimica Acta, 46 (1982) 2381-2393.
[68] M. Kleber, K. Eusterhues, M. Keiluweit, C. Mikutta, R. Mikutta, P.S. Nico, Mineral–organic associations: formation, properties, and relevance in soil environments, in: Advances in agronomy, Elsevier, 2015, pp. 1-140.
[69] J.W. Grate, K.J. Dehoff, M.G. Warner, J.W. Pittman, T.W. Wietsma, C. Zhang, M. Oostrom, Correlation of oil–water and air–water contact angles of diverse silanized surfaces and relationship to fluid interfacial tensions, Langmuir, 28 (2012) 7182-7188.
[70] P.C. Bennett, D. Siegel, M.J. Baedecker, M. Hult, Crude oil in a shallow sand and gravel aquifer—I. Hydrogeology and inorganic geochemistry, Applied Geochemistry, 8 (1993) 529-549.
[71] D. Jones, I. Head, N. Gray, J. Adams, A. Rowan, C. Aitken, B. Bennett, H. Huang, A. Brown, B. Bowler, Crude-oil biodegradation via methanogenesis in subsurface petroleum reservoirs, Nature, 451 (2008) 176-180.
[72] J.J. Zullig, J.W. Morse, Interaction of organic acids with carbonate mineral surfaces in seawater and related solutions: I. Fatty acid adsorption, Geochimica et Cosmochimica Acta, 52 (1988) 1667-1678.
[73] L. Madsen, L. Ida, Adsorption of carboxylic acids on reservoir minerals from organic and aqueous phase, SPE Reservoir Evaluation & Engineering, 1 (1998) 47-51.
[74] P. Jardine, J. McCarthy, N. Weber, Mechanisms of dissolved organic carbon adsorption on soil, Soil Science Society of America Journal, 53 (1989) 1378-1385.
[75] A.W. Adamson, A.P. Gast, Physical chemistry of surfaces, Interscience publishers New York, 1967.
[76] S. Mahdi Jafari, Y. He, B. Bhandari, Nano-emulsion production by sonication and microfluidization—a comparison, International Journal of Food Properties, 9 (2006) 475-485.
[77] S. Dupraz, M. Parmentier, B. Ménez, F. Guyot, Experimental and numerical modeling of bacterially induced pH increase and calcite precipitation in saline aquifers, Chem Geol, 265 (2009) 44-53.
[78] G.M. El-sayed, M. Kamel, N. Morsy, F. Taher, Encapsulation of nano Disperse Red 60 via modified miniemulsion polymerization. I. Preparation and characterization, Journal of applied polymer science, 125 (2012) 1318-1329.
[79] F.U.R. Awan, A. Keshavarz, H. Akhondzadeh, S. Al-Anssari, S. Iglauer, A novel approach for using silica nanoparticles in a proppant pack to fixate coal fines, The APPEA Journal, 60 (2020) 88-96.
[80] S. Ahualli, G. Iglesias, W. Wachter, M. Dulle, D. Minami, O. Glatter, Adsorption of anionic and cationic surfactants on anionic colloids: supercharging and destabilization, Langmuir, 27 (2011) 9182-9192.

[81] F.U.R. Awan, A. Keshavarz, H. Akhondzadeh, S. Al-Anssari, A. Al-Yaseri, A. Nosrati, M. Ali, S. Iglauer, Stable Dispersion of Coal Fines during Hydraulic Fracturing Flowback in Coal Seam Gas Reservoirs—An Experimental Study, Energy & Fuels, 34 (2020) 5566-5577.
[82] R.N. Wenzel, Resistance of solid surfaces to wetting by water, Industrial & Engineering Chemistry, 28 (1936) 988-994.
[83] A.Z. Al-Yaseri, M. Lebedev, A. Barifcani, S. Iglauer, Receding and advancing (CO2+ brine+ quartz) contact angles as a function of pressure, temperature, surface roughness, salt type and salinity, The Journal of Chemical Thermodynamics, 93 (2016) 416-423.
[84] A. Marmur, Soft contact: measurement and interpretation of contact angles, Soft Matter, 2 (2006) 12-17.
[85] L.M. Lander, L.M. Siewierski, W.J. Brittain, E.A. Vogler, A systematic comparison of contact angle methods, Langmuir, 9 (1993) 2237-2239.
[86] I. Gaus, M. Azaroual, I. Czernichowski-Lauriol, Reactive transport modelling of the impact of CO2 injection on the clayey cap rock at Sleipner (North Sea), Chemical Geology, 217 (2005) 319-337.
[87] Y. Hu, Y.-S. Jun, Biotite dissolution in brine at varied temperatures and CO2 pressures: Its activation energy and potential CO2 intercalation, Langmuir, 28 (2012) 14633-14641.
[88] R. El-Maghraby, C. Pentland, S. Iglauer, M. Blunt, A fast method to equilibrate carbon dioxide with brine at high pressure and elevated temperature including solubility measurements, The Journal of Supercritical Fluids, 62 (2012) 55-59.
[89] S. Iglauer, CO2–water–rock wettability: variability, influencing factors, and implications for CO2 geostorage, Accounts of Chemical Research, 50 (2017) 1134-1142.
[90] M. Arif, S.A. Abu-Khamsin, S. Iglauer, Wettability of rock/CO2/brine and rock/oil/CO2-enriched-brine systems: Critical parametric analysis and future outlook, Advances in colloid and interface science, 268 (2019) 91-113.
[91] A. Abramov, A. Keshavarz, S. Iglauer, Wettability of Fully Hydroxylated and Alkylated (001) α-Quartz Surface in Carbon Dioxide Atmosphere, The Journal of Physical Chemistry C, 123 (2019) 9027-9040.
[92] I. Nowrouzi, A.K. Manshad, A.H. Mohammadi, Effects of TiO2, MgO and γ-Al2O3 nano-particles on wettability alteration and oil production under carbonated nano-fluid imbibition in carbonate oil reservoirs, Fuel, 259 (2020) 116110.
[93] M. Ali, S. Al-Anssari, M. Shakeel, M. Arif, N.U. Dahraj, S. Iglauer, Influence of Miscible CO 2 Flooding on Wettability and Asphaltene Precipitation in Indiana Lime Stone, in: SPE/IATMI Asia Pacific Oil & Gas Conference and Exhibition, Society of Petroleum Engineers, 2017.
[94] M. Ali, N.U. Dahraj, S.A. Haider, Study of Asphaltene Precipitation during CO2 Injection in Light Oil Reservoirs, in: SPE/PAPG Pakistan section Annual Technical Conference, Society of Petroleum Engineers, 2015.

Conflict of Interest

Declaration of interests

☒ The authors declare that they have no known competing financial interests or personal relationships that could have appeared to influence the work reported in this paper.

☐The authors declare the following financial interests/personal relationships which may be considered as potential competing interests:

Author Statement

Muhammad Ali: Conceptualization, Methodology, Validation, Formal analysis, Investigation, Data Curation, Writing - Original Draft, Writing - Review & Editing

Adnan Aftab: Data Curation, Visualization

Faisal Ur Rehman Awan: Formal analysis, Methodology

Hamed Akhondzadeh: Software, Data Curation

Alireza Keshavarz: Methodology, Validation, Writing - Review & Editing

Ali Saeedi: Methodology, Validation, Writing - Review & Editing, Supervision

Stefan Iglauer: Conceptualization, Methodology, Validation, Writing - Review & Editing, Supervision

Mohammad Sarmadivaleh: Conceptualization, Methodology, Resources, Writing - Review & Editing, Project administration, Supervision